



## An Impregnation Route to Synthesis of BiVO<sub>4</sub>/NaY Materials and Photocatalytic Activities under Visible Light Irradiation†

XIAOWEN XU\* and QIUYANG NI

Department of Chemistry, Jiangsu Key Laboratory for Environment Functional Materials, Suzhou University of Science and Technology, Suzhou 215011, P.R. China

\*Corresponding author: E-mail: xwxu@mail.usts.edu.cn

Published online: 1 March 2014;

AJC-14782

Bismuth vanadate (BiVO<sub>4</sub>) nanoparticles were prepared on NaY type zeolite by impregnation with Bi(NO<sub>3</sub>)<sub>3</sub> and NH<sub>4</sub>VO<sub>3</sub> solution and subsequent calcination at different temperatures. The materials consist of BiVO<sub>4</sub> nano-crystals with average size of 7 nm and NaY zeolite, described as BiVO<sub>4</sub>/NaY (BV), show a strong absorption in the visible light region. The powders were tested by degradation of methyl orange with  $\lambda > 400$  nm light, which was found to have significantly superior photocatalytic activity compared to BiVO<sub>4</sub>.

**Keywords:** Nano-crystalline materials, Zeolite, BiVO<sub>4</sub>, Catalysis.

### INTRODUCTION

Bismuth vanadate (BiVO<sub>4</sub>) is well-known for its ferro-elastic properties and its use as a nontoxic, bright yellow pigment and has received some attention as a visible-light active photocatalyst. A number of approaches, such as co-precipitation, hydrothermal treatment, electrodeposition method and sol-gel method, have been developed to synthesize mBiVO<sub>4</sub><sup>1-4</sup>. With a narrow bandgap, BiVO<sub>4</sub> has shown significant visible-light activity for degradation contamination under visible light irradiation, which act as oxidizing agent<sup>5</sup>. Zeolites have been used as a host for the growth of nano-particles on the external surface of zeolite. Zhang *et al.*<sup>6</sup> synthesized BiVO<sub>4</sub>-MCM-41 composite catalyst, which is supporting BiVO<sub>4</sub> with monoclinic Scheelite structure on the surface of MCM-41 molecular sieve. We also have reported that the Bi<sub>2</sub>MoO<sub>6</sub> nanoparticles formed on the external surface of NaY zeolite<sup>7</sup>. The nano-particles supported on external surface of zeolites are favorable to contact with reactive molecules for catalysis. In this study, we report a facile impregnation route for the synthesis of BiVO<sub>4</sub>/NaY (BV) photocatalyst, supporting the BiVO<sub>4</sub> nanoparticles on the surface of the NaY zeolite, to improve the photocatalytic activities.

### EXPERIMENTAL

All reagents used in the present experiments were of analytical purity from commercial sources. The photocatalyst

was synthesized using bismuth nitrate [Bi(NO<sub>3</sub>)<sub>3</sub>·5H<sub>2</sub>O] as bismuth source and ammonium metavanadate (NH<sub>4</sub>VO<sub>3</sub>) as vanadium source. Aqueous solutions of Bi(NO<sub>3</sub>)<sub>3</sub>·5H<sub>2</sub>O and NH<sub>4</sub>VO<sub>3</sub> were 1:1 molar ratio. The temperature was maintained at 323 K throughout the whole preparation process. A typical synthesis process is as follows: 1.9403 g Bi(NO<sub>3</sub>)<sub>3</sub>·5H<sub>2</sub>O was dissolved in 10 mL distilled water to get solution of Bi(NO<sub>3</sub>)<sub>3</sub>, then 1.000g NaY (Si/Al = 1.6) was impregnated with the above solution under vigorous stirring for 15 min and then dropped 0.4679 g NH<sub>4</sub>VO<sub>3</sub> into the suspension. During the co-precipitation step, the pH of the mixed solution was adjusted to five using an aqueous ammonia solution. After stirring for 0.5 h, the precipitate was centrifugated and the resulting product was thoroughly washed with distilled water to remove remained nitrogen to purify the precursor. The as-synthesized materials were calcined at 393, 473, 573 and 673 K in an oven for 2 h with a heating rate of 20 K/min and then cooled to ambient temperature to give BV-393, BV-473, BV-573 and BV-673 (BV stands for BiVO<sub>4</sub>/NaY and the number indicates the temperature of calcination), respectively. For comparison, BiVO<sub>4</sub> powders were prepared at 673 K using analogous means and increasing the load content of BiVO<sub>4</sub> to 3 times compared to above reference, the corresponding products sign as BV-393 (high), BV-473 (high), BV-573 (high) and BV-673 (high).

†Presented at The 7th International Conference on Multi-functional Materials and Applications, held on 22-24 November 2013, Anhui University of Science & Technology, Huainan, Anhui Province, P.R. China

## RESULTS AND DISCUSSION

**Characterization:** The crystal structure of the catalysts was characterized by X-ray diffraction (XRD) measurements, which was conducted with a Bruker D8 Advance diffractometer with  $\text{CuK}\alpha$  radiation over a  $2\theta$  range from  $5\text{--}60^\circ$  and operated at 45 kV and 20 mA with a scan rate of  $4^\circ/\text{min}$  and step size of  $0.02^\circ$ . The sample size and morphology was examined by transmission electron microscope (TEM) using a JEOL JEM-1200EX instrument operating at 120 kV. The optical properties were measured using Hitachi U-3010 UV-VIS spectrophotometer.

**Photocatalytic activity of samples:** Photocatalytic activities were measured by degradation of methyl orange in aqueous solutions under visible light. Photocatalytic reactions were run in 250 mL glass beaker of a 20 mL, 10 mg/L methyl orange solution contained 0.10 g catalyst and were stirred for 0.5 h before the light was turned on to ensure adsorption/desorption equilibrium between the catalyst and the solution. Then the solution was irradiated for different time under vigorous stirring by using a 400 W Xe lamp (CTXE-450, adjustable) as the visible light source. The distance between reactant and light source was remained at 25 cm. Cutoff filters (Hoya) were employed for controlling the wavelength of incident light.

From Fig. 1A, the XRD patterns of the  $\text{BiVO}_4$  and BV calcined at different temperatures show that the characteristic peaks of NaY is relatively weak and absent of the characteristic peaks of  $\text{BiVO}_4$ . This reason may be that the characteristic peaks of  $\text{BiVO}_4$  were inundated by that of NaY. The XRD pattern of  $\text{BiVO}_4$  (Fig. 1f) shows a pair of peaks at  $2\theta = 19.04, 28.96, 30.6, 35.26, 39.88$  and  $53.28^\circ$ , which are ascribed to monoclinic  $\text{BiVO}_4$ <sup>6</sup>.

Fig. 1B presents the XRD patterns of the  $\text{BiVO}_4$  and BV (high) calcined at different temperatures. As can be seen in Fig. 1B, the characteristic peaks of  $\text{BiVO}_4$  were obviously observed, but the characteristic peaks of NaY were relatively weak compared to the characteristic peaks in Fig. 1A. The diffraction intensity of  $\text{BiVO}_4$  characteristic peaks in the XRD pattern of BV (high) is much weaker and broader than that of  $\text{BiVO}_4$  (Fig. 1f). The fact implies that  $\text{BiVO}_4$  nanoparticles have formed on the zeolite.

TEM micrographs (Fig. 2a) clearly show  $\text{BiVO}_4$  extremely high dispersed on the outer surface of NaY zeolite single crystallites and  $\text{BiVO}_4$  consists of relative uniform microspheres with a diameter of 7 nm, which is about 100 times smaller than NaY zeolite. Fig. 2c shows that the  $\text{BiVO}_4$  nanoparticles with the size of about 10 nm formed on the outer surface of NaY zeolite single crystallites. Interestingly, as it is seen in Fig. 2b, the particles of  $\text{BiVO}_4$  on NaY type zeolite are composed of many smaller particles. On increasing the load content of  $\text{BiVO}_4$  to 3 times, the  $\text{BiVO}_4$  was not highly dispersed on NaY zeolite surface and accumulated on NaY zeolite surface. The fact indicates that increasing the relative content of  $\text{BiVO}_4$  in BV is disadvantaged of the dispersion of  $\text{BiVO}_4$  on the NaY zeolite surface.

EDAX patterns (Fig. 2d and e) show that the content of Bi atoms is higher than that of V atoms according to the molar ratio of Bi and Mo is 1:1. This phenomenon may be attributed to that some of the  $\text{BiO}^+$  or  $\text{Bi}^{3+}$  are in the channel of the zeolite

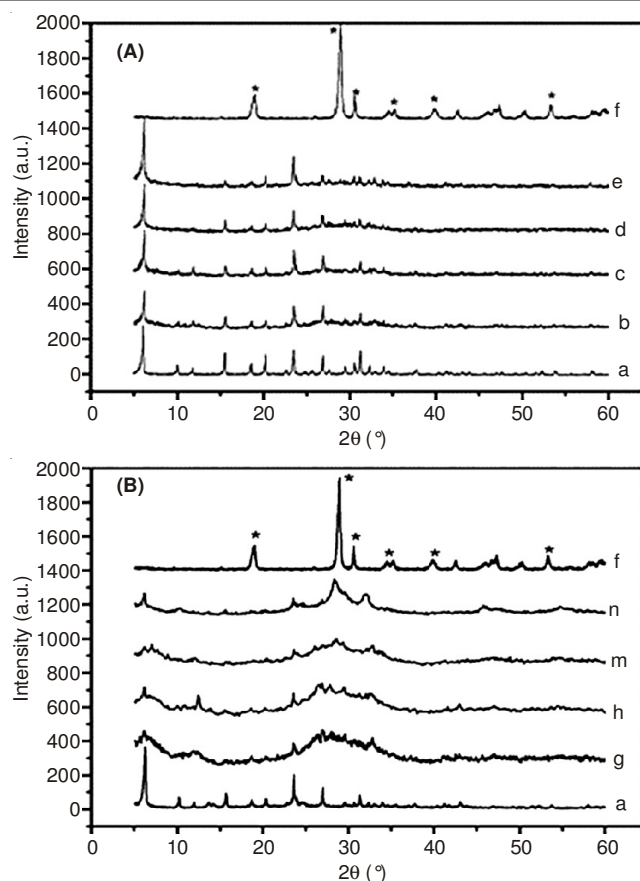


Fig. 1. (A) XRD pattern of (a) NaY, (b) BV-393, (c) BV-473, (d) BV-573, (e) BV-673, (f)  $\text{BiVO}_4$ ; (B) XRD pattern of (a) NaY, (g) BV-393 (high), (h) BV-473 (high), (m) BV-573 (high), (n) BV-673 (high), (f)  $\text{BiVO}_4$  (the \* indicate the characteristic peaks of  $\text{BiVO}_4$ )

by ion exchange and do not integrate with  $\text{VO}_3^-$ , indicating that  $\text{BiO}^+$  and  $\text{VO}_3^-$  were not completely precipitated. The equation of the co-precipitation as follows:

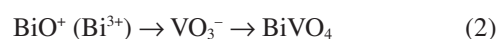
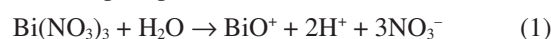


Fig. 3 represents the diffuse reflectance spectra of  $\text{BiVO}_4$  prepared at 673 K and BV prepared at different temperature. All of the products show excellent visible light absorption and  $\text{BiVO}_4$  shows the best visible light response. But for BV (Fig. 3a-d) materials, the characteristic absorption band in visible light region is weaker compared to  $\text{BiVO}_4$  (Fig. 3e) and the temperature only influence the absorbance intensity in UV region. This is probably the reason that the inverse proportion of  $\text{BiVO}_4$  in BV materials is small, which influencing the BV to absorb visible light and the crystalline structure would not change with increasing the temperature. But for the higher load  $\text{BiVO}_4$  (Fig. 3B), the diffuse reflectance spectra have not obvious difference. This implied that the load content, the calcined temperature did not influence the diffuse reflectance spectra of  $\text{BiVO}_4$ .

Based on extrapolations of the straight portions of the absorption edge, it can be estimated that BV and  $\text{BiVO}_4$  have a band gap of 2.4 eV, which can be ascribed to the characteristic absorption of monoclinic  $\text{BiVO}_4$ <sup>8</sup>. The visible light absorption can be accounted for the transition of covalent band formed by Bi 6s or Bi 6s and O 2p hybrid orbitals towards V 3d<sup>8</sup>. The

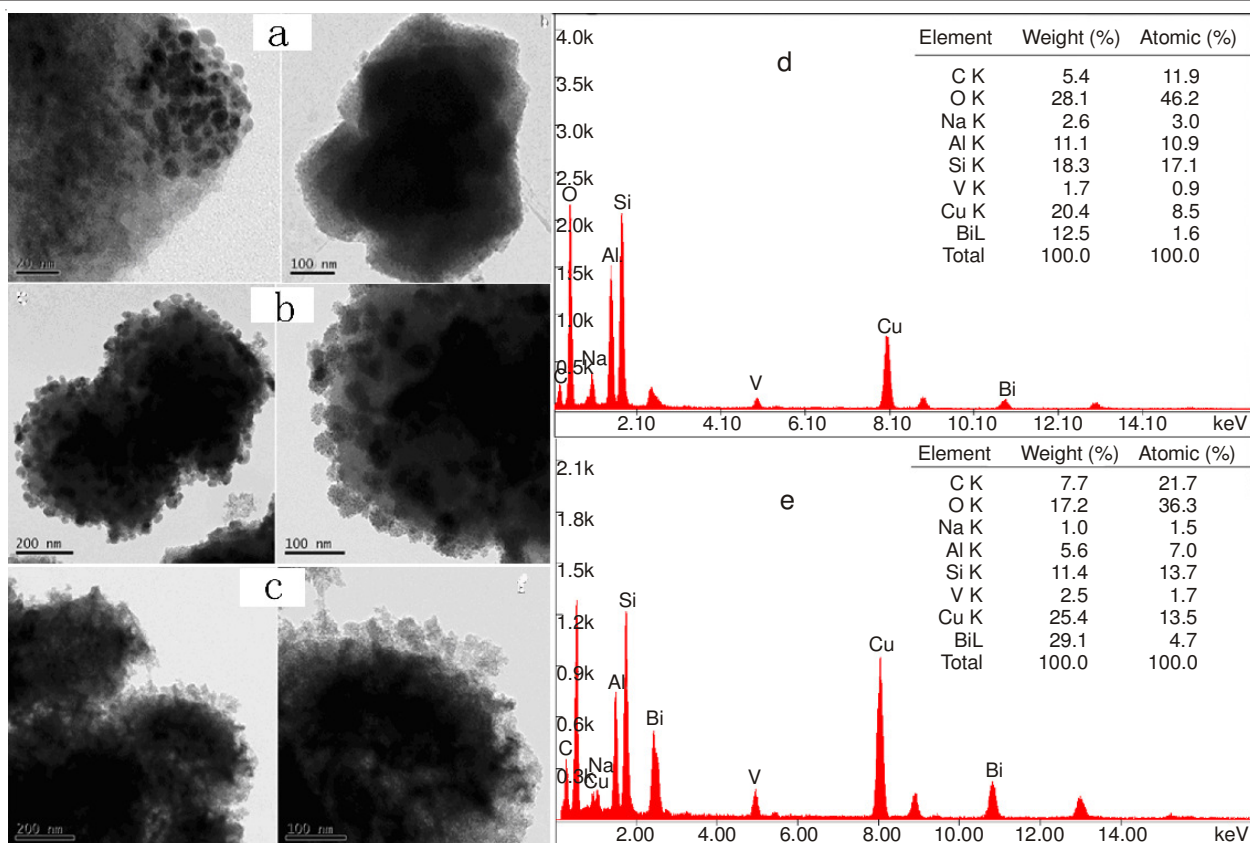


Fig. 2. TEM images of (a) BV-673, (b) BV-393(high), (c) BV-673(high) and the EDAX patterns of (d) BV-393(high), (e) BV-673(high)

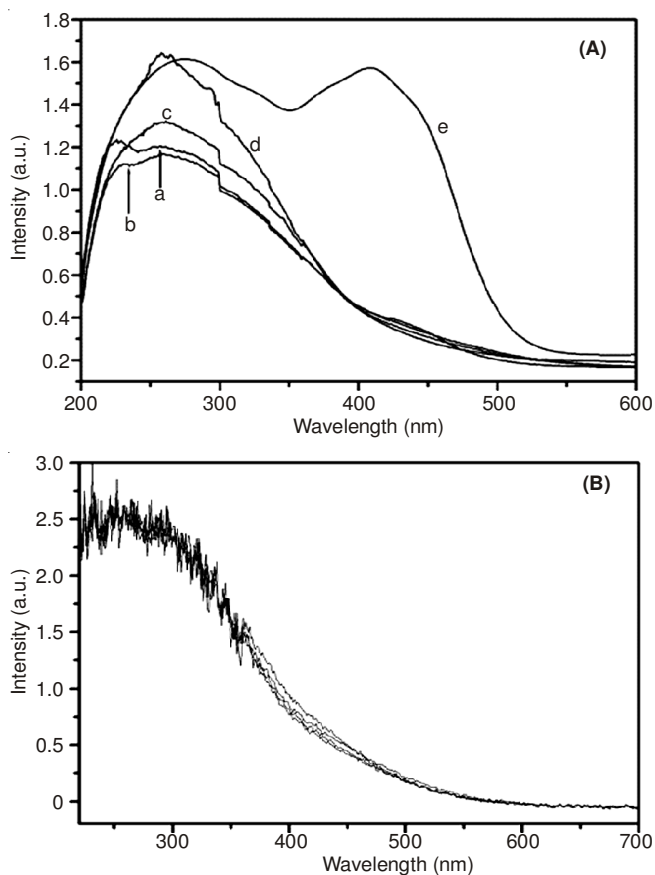


Fig. 3. (A) Diffuse reflectance spectra of (a) BV-393, (b) BV-473, (c) BV-573, (d) BV-673, (e) BiVO<sub>4</sub>. (B) Diffuse reflectance spectra of NaY and BV (high load)

sharp peaks on spectra (Fig. 3e) show that visible absorption of BiVO<sub>4</sub> is transited from forbidden band instead of pure state. This resulted in a direct band gap semiconductor with a smaller band gap and enhanced visible light absorption<sup>6</sup>.

Fig. 4 shows the results of photocatalytic experiments with the above-mentioned oxides irradiated with  $\lambda > 400$  nm light. The BV-673 possessed a high photocatalytic activity under visible light irradiation, as shown in Fig. 4A. The photocatalytic activity of BV-673 results in a photocatalyst that is roughly three times more active than BV-573 and BiVO<sub>4</sub>, which is the most commonly used as photocatalyst for degradation organic contamination and about two times more active than BV-473 and BV-393. The improved activity is not due to the characteristic absorption band in the visible light region, since all of the catalysts have absorption in visible light region. Such a large activity enhancement probably arises from the extent of crystallinity and with increasing the temperature the contents of the impurities decreased, which benefit to the photocatalytic properties<sup>9</sup>. But keeping on increasing the temperature, the particle size increased also, which lead to the lower specific surface area and then probably the lower photocatalytic activity.

From Fig. 4B, the higher load BiVO<sub>4</sub> have lower photocatalysis, indicating that increasing the relative content of BiVO<sub>4</sub> in BV compounds was disadvantaged for the photocatalysis. This may be the reason that the BiVO<sub>4</sub> on the NaY zeolite surface was not highly dispersion (Fig. 2b,c) and would not effectively reacted with methyl orange molecule.

In this study we observed nanoparticles of ternary metal oxide formed on the outer surface of NaY zeolite crystallites. The phenomena observed are not able to be understood with

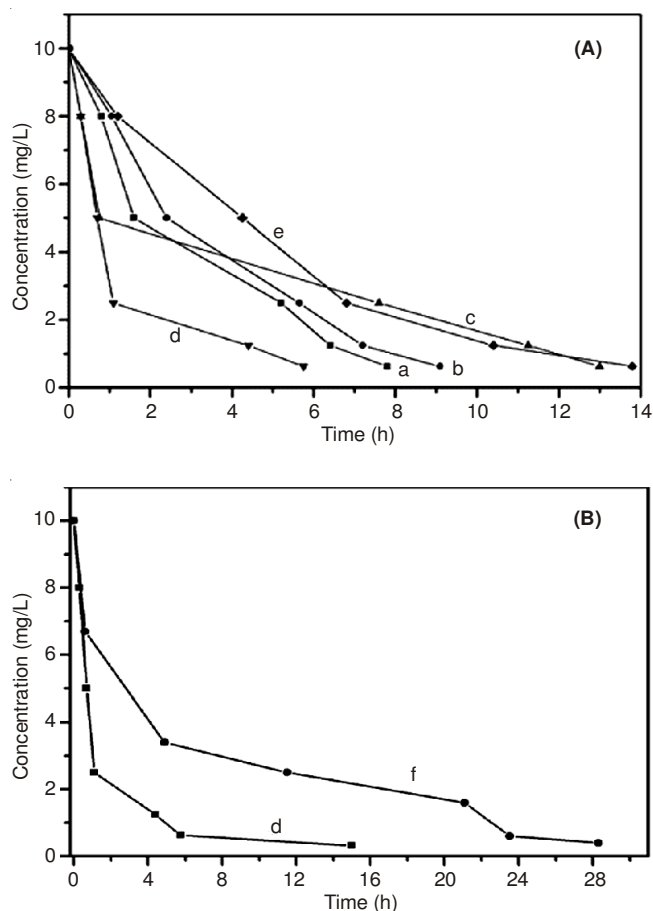


Fig. 4. (A) Patterns of powers decomposition of methyl orange under visible light. (a) BV-393, (b) BV-473, (c) BV-573, (d) BV-673, (e) BiVO<sub>4</sub> (B) Patterns of powers decomposition of methyl orange under visible light. (d) BV-673, (f) BV-673 (high)

the principles by Xie and Tang<sup>10</sup>. No perfect and pure Si-O bonds exist on the surface of a zeolite with 1.6 of framework

Si/Al ratio. Actually, partly ionic bonds between the cations and the Si-O-Al-O surface of the zeolite lead to ion exchange to form monolayers of BiO<sup>+</sup> or Bi<sup>3+</sup> on the zeolite. When the solution of NH<sub>4</sub>VO<sub>3</sub> was dropped, VO<sub>3</sub><sup>-</sup> dispersed on the surface of the zeolite, the co-precipitation occurred. On the basis of the above analysis, it can be concluded that the surface of the zeolite with low Si/Al ratios plays a role in forming BiVO<sub>4</sub>, which greatly increases the possibility of forming BiVO<sub>4</sub> nanoparticles on the zeolite surface. Therefore, we believe that our method should be applicable to growth ternary metal oxide nanoparticles on the zeolite with low Si/Al ratios, so the fields in photocatalysts may be greatly expanded.

We have developed a facile and economical method to produce BV on a large scale. This method has the potential use in preparation of other complex oxide photocatalysts with small particle size.

## REFERENCES

1. U.M. García-Pérez, S. Sepúlveda-Guzmán and A. Martínez-de-la Cruz, *Solid State Sci.*, **14**, 293 (2012).
2. F. Lin, D.G. Wang, Z.X. Jiang, Y. Ma, J. Li, R. Li and C. Li, *Energy Environ. Sci.*, **5**, 6400 (2012).
3. K.J. McDonald and K.-S. Choi, *Energy Environ. Sci.*, **5**, 8553 (2012).
4. H. Liu, R. Nakamura and Y. Nakato, *J. Electrochem. Soc.*, **152**, 856 (2005).
5. C. Yin, S.M. Zhu, Z.X. Chen, W. Zhang, J.J. Gu and D. Zhang, *J. Mater. Chem. A*, 8367 (2013).
6. L. Zheng, L. Xiong, J. Sun, J. Li, S. Yang and J. Xia, *Chin. J. Catal.*, **29**, 624 (2008).
7. X.W. Xu and Q.Y. Ni, *Catal. Commun.*, **11**, 359 (2010).
8. D.N. Ke, T.Y. Peng, L. Ma, P. Cai and K. Dai, *Inorg. Chem.*, **48**, 4685 (2009).
9. S.C. Zhang, C. Zhang, Y. Man and Y. Zhu, *J. Solid State Chem.*, **179**, 62 (2006).
10. Y. Xie and Y. Tang, *Adv. Catal.*, **37**, 1 (1990).